



# Sampling and diversion strategy for twin-screw granulation lines using batch statistical process monitoring

Fanny Stauffer<sup>a,\*</sup>, Eliot Boulanger<sup>b</sup>, Gabrielle Pilcer<sup>a</sup>

<sup>a</sup> Product Design & Performance, Pharma Sciences, UCB, Braine l'Alleud, Belgium

<sup>b</sup> Biotech Digital Sciences, Biotech Sciences, UCB, Braine l'Alleud, Belgium

## ARTICLE INFO

### Keywords:

Continuous manufacturing  
Granulation  
Pharmaceutical process  
Process control  
Quality-by-design

## ABSTRACT

Continuous manufacturing is now considered as a well-established technique by pharmaceutical companies. However, the limited number of filed applications reflects the complexity to translate a science that has been described in many publications to an actual drug product. Process stability evaluation and resulting sampling and diversion strategy are key aspects of the design of continuous processes which require the development of new approaches. This study describes a new methodology to evaluate process stability for a continuous line based on twin-screw granulation. In such lines, both continuous and discrete unit operations are present. The diversion and quality decision of intermediate product is therefore made at the level of individualized portions of the batch called product keys (PK). The described methodology therefore evaluates the process stability at PK level. A batch statistical process model was calibrated with three manufacturing campaigns and verified on five independent campaigns. The developed model allowed identifying outlying PKs within a manufacturing campaign. This approach gives new perspectives for rationalizing the sampling strategy, designing the diversion strategy and continued process verification. Further extension of the model could be considered to enable its use for quality decision.

## 1. Introduction

Continuous manufacturing technology is now well established in a number of pharmaceutical companies. The most common drug product processes, in particular (i.e. wet granulation, dry granulation, direct compression), have been redesigned to be integrated into continuous manufacturing lines. However, since the publication of the Food and Drug Administration (FDA) guidance for Process Analytical technology (PAT) in 2004 (Food and Drug Administration 2004), only seven industrial applications of such technology have been deployed for a product reaching the market (Vanhoorne and Vervaet, 2020). This limited number of instances highlights the complexity of developing the scientific understanding and to apply this innovative approach to actual products.

Most papers on continuous manufacturing are considering a single unit operation and / or are focusing of the identification of Critical Process Parameters (CPP). While this aspect is often easily covered during process development (International Conference on 2009), the main industrial challenge when considering such technique is to ensure that the developed process is robust and stable over time (Vercauysse

et al., 2013, Stauffer et al., 2019). In order to fully benefit from the advantages of continuous manufacturing during development, the design space is usually defined on short manufacturing runs that are assumed to be representative of the process at any point in time (Byrn et al., 2014, Lee et al., 2015, Plumb, 2005, Vervaet et al., 2013). The stability of the process at the considered set point should then be demonstrated to ensure that the product quality is consistent over time (International Conference on 2008). This evaluation is the corner stone of the definition of a control strategy. The draft FDA guidance on Quality Considerations for Continuous Manufacturing (Food and Drug Administration 2019) and the draft ICH Q13 guideline on continuous manufacturing (International Conference on 2021) especially emphasize on the understanding of process dynamics and variability and the need to develop suitable strategy for this evaluation. Multivariate approaches are perceived as the most suitable tools to capture intra-batch and inter-batch variation. The same approach can also be extended to commercial manufacturing for continued process verification (CPV) to provide continual insurance that the process remains in a state of control.

In this study, we investigated the intra-batch and inter-batch

\* Corresponding author.

E-mail address: [fanny.stauffer@ucb.com](mailto:fanny.stauffer@ucb.com) (F. Stauffer).

<https://doi.org/10.1016/j.ejps.2022.106126>

Received 30 September 2021; Received in revised form 21 December 2021; Accepted 12 January 2022

Available online 21 January 2022

0928-0987/© 2022 Published by Elsevier B.V. This is an open access article under the CC BY-NC-ND license (<http://creativecommons.org/licenses/by-nc-nd/4.0/>).

**Table 1**  
 Repartition of raw materials batches for the different manufacturing campaign (run) used in this study.

Campaign run	API batch	Excipients batch
Cal1	API-A	Exc-A
Cal2	API-B	Exc-B
Cal3	API-B	Exc-B
V1	API-A	Exc-A
V2	API-C	Exc-B
V3	API-C	Exc-B
V4	API-B	Exc-B
V5	API-D	Exc-C

**Table 2**  
 List of monitored process parameters.

Process step	Process parameter	Acceptable range
Feeding	Powder flow rate	Acceptable range
	Weight in the feeder	20 kg/h [8; 25]
	Screw speed	> 0.7 kg
Granulation	Liquid mass flow	N/A
	L/S ratio	N/A
	Screw speed	32% [26.5; 35.0]
	Torque	600 rpm [300; 900]
	Barrel temperature	N/A
	Jacket liquid temperature	25 °C [25; 40 °C]
	Wet transfer flow	N/A
Drying	Pressure drop granulator outlet	N/A
	Drying time per dryer cell	N/A
	Air inlet temperature	< 1000 s
	Air inlet humidity	72 °C [70; 80]
	Air velocity	N/A
	Product temperature per cell	360 m <sup>3</sup> /h [360; 380]
	ΔT per dryer cell	N/A
	Pressure difference air distribution plate	20 °C [16; 30]
	Pressure difference dryer filters	< 6 %
	Pressure difference Volkmann	< 70 mbar
Pneumatic transfer		
Milling	Mill speed	N/A

variation of a continuous process based on twin-screw granulation. The process was continuous from pre-blend feeding to milling and was developed for a ConSigma-25 line. The continuous manufacturing line was composed of a feeder, a twin-screw granulator, a six-segmented fluid-bed dryer and a conical mill. Current literature investigating the stability and robustness of this line are either relying on intensive sampling of intermediates and of the final product (Vercausse et al., 2013) or multivariate statistical process control (MSPC) based on process sensors exclusively (Silva et al., 2017, Zomer et al., 2018) or in combination with in-line PAT data (Roggo et al., 2020). The use of MSPC showed to be efficient in understanding process dynamics and deviations. However, as highlighted by Fonteyne et al. in their detailed description of the equipment (Fonteyne et al., 2012), even though the considered process is a continuous one, the dryer and milling units operates with individualized portions of the batch that experience a transient transformation. These individualized portions of the batch, also called product key (PK), are going through granulation, drying and milling. A quality decision is taken on each PK: conforming PKs are progressing to final blending, while non-conforming PKs are discarded from the process after milling. Two types of MSPC models have been described on this process line. While Zomer et al. (2018) acknowledged the discrete nature of the drying operation, the model they developed considered the dryer unit as a continuous operation by averaging over the process values of the PKs inside the dryer. This approach allows for an overview on how the process is running but is not able to detect a deviation at PK level. Another method was suggested by Silva et al. (2018) by using batch statistical process monitoring (BSPM) instead of

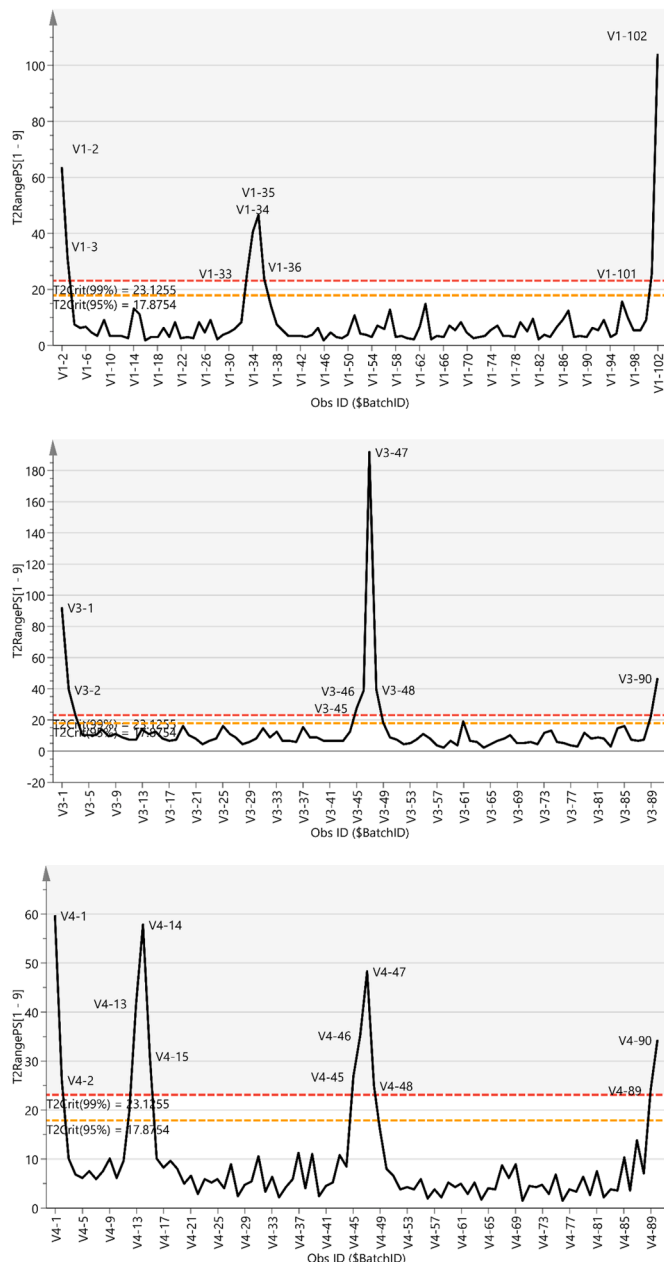


**Fig. 1.** Hotelling's T<sup>2</sup> control chart of test campaigns V1 (top), V3 (middle) and V4 (bottom). The x-axis represents the sequence of PK per campaign. Deviating PKs are labeled.

MSPC to detect deviations at the individual PK level. This approach focuses on the batch evolution model (BEM) to detect deviations within a PK and considers only the drying of a PK. We propose here an approach that intends to leverage the best of both worlds by considering the process at PK level and by accounting for all the unit operations (i.e. granulation, drying and milling). This way, this single model could be used to determine deviating PKs, enabling CPV at PK level and use of this model for diversion strategy.

This paper describes the use of BSPM to identify non-conforming PKs. This methodology will be exemplified by an application to an industrial case study for which the model could trigger the diversion of non-conforming PKs.

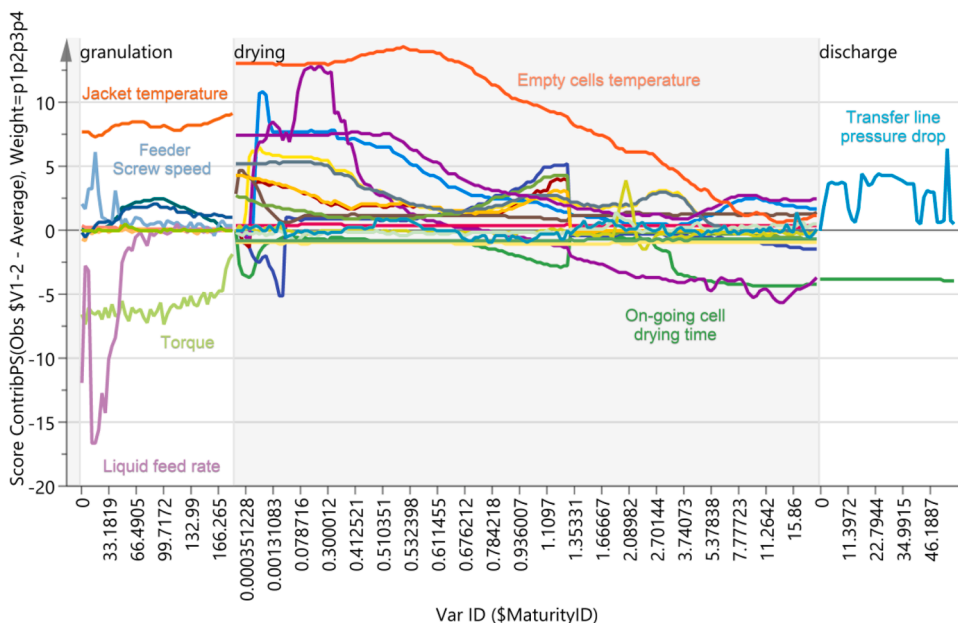


Fig. 2. Contribution plot – Start up (average of V1-2 and 3, V3-1 and 2, V4-1 and 2). The x-axis represents the aligned time series expressed as dryer cell filling time for the granulation, deltaT for the drying phase and discharge time for the discharge phase.

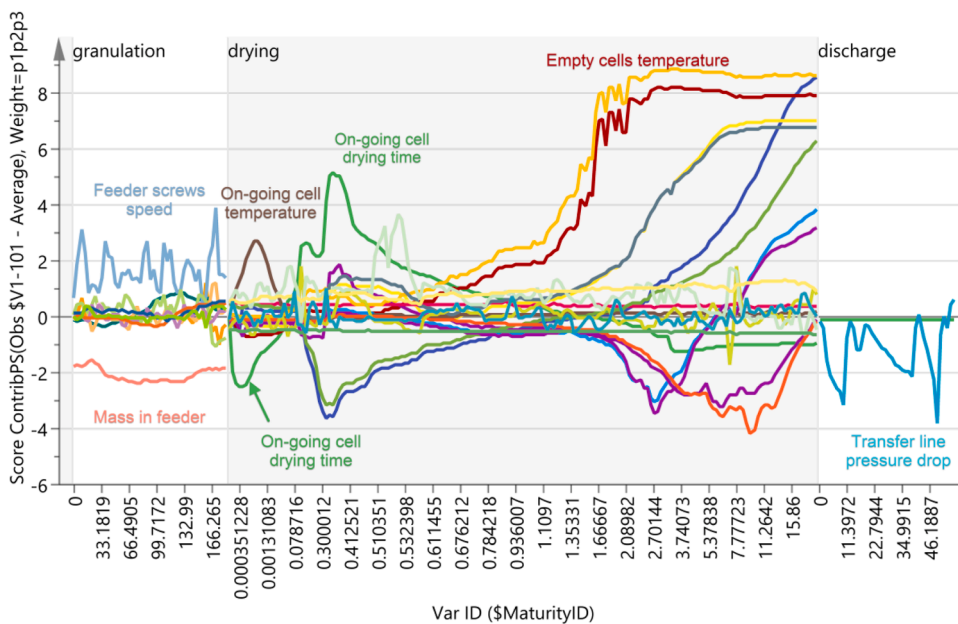


Fig. 3. Contribution plot –Shut down (average of V1-101 and 102, V3-90, V4-89 and 90). The x-axis represents the aligned time series expressed as dryer cell filling time for the granulation, deltaT for the drying phase and discharge time for the discharge phase.

2. Materials and methods

2.1. Materials

The powder blends used in this study consisted of 40.0% of an active ingredient under development, 34.8% of lactose monohydrate (Pharmatose 200 M, DFE pharma, Hemiksem, Belgium), 17.2% of microcrystalline cellulose (Avicel PH102, DuPont Pharma, Dange Saint Romain, France), 4.0% of Hypromellose 2910 (Methocel E3, Ashland, Schaffhausen, Switzerland) and 4.0% of sodium croscarmellose (Ac-Di-Sol, DuPont Pharma, Dange Saint Romain, France). Purified water was used as granulation liquid.

Granules were produced during eight independent manufacturing

campaign spread over seven months, three were used as reference campaigns for model construction and five as tests campaigns for model assessment. Batches of raw materials were then distributed between the runs as shown in Table 1.

2.2. Manufacturing process

The API could not be fed directly to a continuous blender due to its poor flowability. A batch blending process step was, therefore, chosen for blending the intra-granular ingredients. Batch size varied between 21 and 102 kg to accommodate for the supply needs. Raw materials were first sieved using a conical mill (Comil, Quadro, Waterloo, Canada) on a 2 mm screen and transferred into a bin of appropriate size.

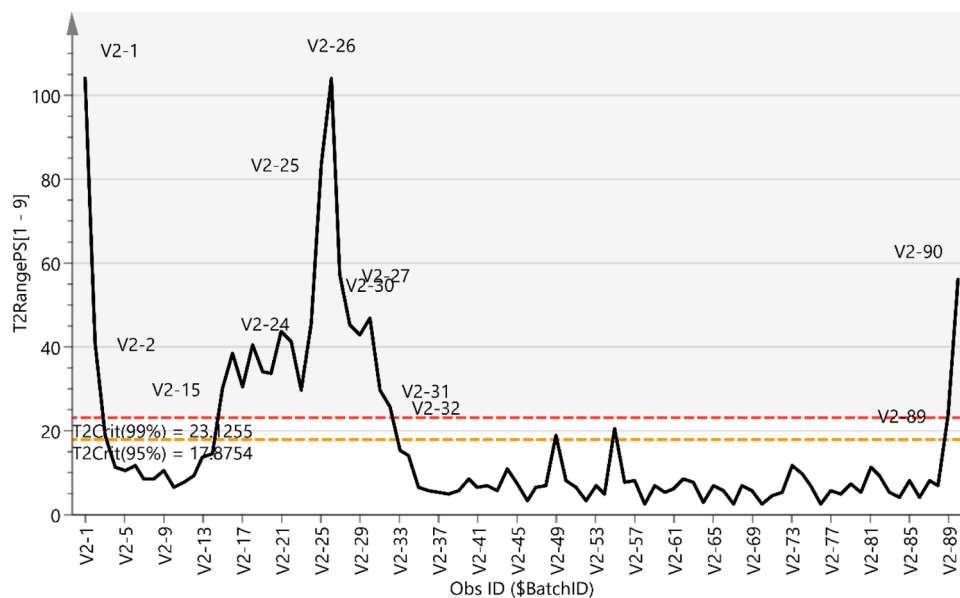


Fig. 4. Hotelling's  $T^2$  control chart of test campaign V2. The x-axis represents the sequence of PK per campaign. Deviating PKs are labeled.

The intra-granular ingredients were blended for 30 min at 10 rpm. Blend homogeneity was assessed before production.

Granules were produced using a Consigma 25 line (GEA engineering, Wommelgem, Belgium) (Fonteyne et al., 2013). The pre-blend was fed into the twin-screw granulator using a continuous twin-screw feeder and automatic refilling. The powder feed rate was set to 20 kg/h. The temperature of the cooling jacket around the granulator barrel was kept constant at 25 °C. The granulator was mounted with a  $2 \times 6$  screw configuration composed of two kneading zones of each six kneading elements at 60° stagger angle (Vercurryse et al., 2012). The screw speed was set to 600 rpm and the liquid-to-solid (L/S) ratio to 32%.

After granulation, the wet granules were gravimetrically transferred to a six-segmented fluid bed dryer which working mechanism was described in detail by De Leersnyder et al. (2018). The air inlet temperature was set to 72 °C and the air velocity to 360 m<sup>3</sup>/h. These values could be adjusted by the operator between 70 and 80 °C and 360 and 380 m<sup>3</sup>/h during the run to accommodate for lack of fluidization or too long drying time if needed. Though the air inlet humidity was not accurately controlled, the air conditioning unit was set to ensure that the air inlet humidity would not exceed 6% relative humidity. The dryer was cleaned and pre-heated before starting the granulation to ensure that inlet air temperature, humidity and air velocity are at steady state from the beginning of each run. The granule mass in one dryer cell is defined as a product key (PK). The PK mass was determined by the powder feed rate (20 kg/h) and the cell filling time (3 min) resulting in PK theoretical mass of 1 kg. The drying end point was determined by the granule temperature increase in each cell ( $\Delta T$ ). This value was set to 20 °C and could be adjusted by the operator between 16 and 30 °C based on at-line residual moisture content and drying time. In case the defined  $\Delta T$  was not achieved in less than 1000s, the end point was triggered by the drying time instead of  $\Delta T$ .

When the drying end point was reached, the fluid-bed dried granules were discharged from the dryer and pneumatically transferred to the mill through a dry transfer line. The mill was mounted with a 1016  $\mu\text{m}$  grater screen. The mill speed was set to 1000 rpm.

The production line was equipped with multiple sensors which allow for the online monitoring of the process. Sensors measured user-set controlled variables (e.g., feed rates, air velocity) and uncontrolled variables (e.g. granulator torque). Process parameters used to build the batch model are listed in Table 2. Based on previous evaluations to assess the sampling frequency to obtain a suitable noise-to-signal ratio

for the different parameter values, feeding and granulation parameters were recorded every 2 s, drying parameters every 4 s and discharge parameters every 1 s.

### 2.3. Development of the batch model

The batch statistical model (BSP) was developed and evaluated using Simca software (Version 14.0.0, Umetrics, Umeå, Sweden). The process data listed in Table 2 were used to build the model.

Previous studies using MSPC on data coming from a Consigma line were either considering a continuous process from feeding to milling / tableting (Silva et al., 2017, Zomer et al., 2018) or a batch process taking only into account the drying step (Silva et al., 2018). In this study a batch model was built, encompassing the feeding, granulation, drying and pneumatic transfer steps. These different phases were split based on the following logic: a feeding – granulation phase driven by the dryer cell filling time, a drying phase driven by the  $\Delta T$  in the cell of interest and a transfer phase driven by the discharge time. For the model, each PK was considered as a batch in the sense of MSPC modeling. To enable this approach, data pre-treatment was needed to individualize the PKs and to properly identify the different phases. The data preparation phase was done using Python 3 scripts. It has to be noticed that Python was used for the proof of concept but is not the end solution considered for the future GMP environment. First, the different PKs were identified based on their recorded drying time (which also includes the cell filling time). When a PK enters the dryer this value start increasing with a starting value of 0. The PK processing through the considered steps is finished when drying time drops back to zero. Up to six PKs are processed (due to the 6 segment of the dryer) and the corresponding data is recorded in parallel. To identify the different PKs, it is important to know in which phase a given PK is. These phases have therefore been identified for each PK. A PK was considered as in granulation phase for as long as the cell filling time is increasing. It was considered as in its drying phase from the start of the granulation (granulation and initial drying occurring simultaneously) to the start of the discharge. The discharge starts when a significant pressure drop in the pneumatic transfer line (GCU\_VH) is observed and this until it returns to normal. As the dryer is composed of six segments operating in parallel, six segment temperatures are recorded at each point in time, their name being defined by the cell physical position in the dryer ranging from 1 to 6. The cell temperatures needed to be extracted to isolate the data

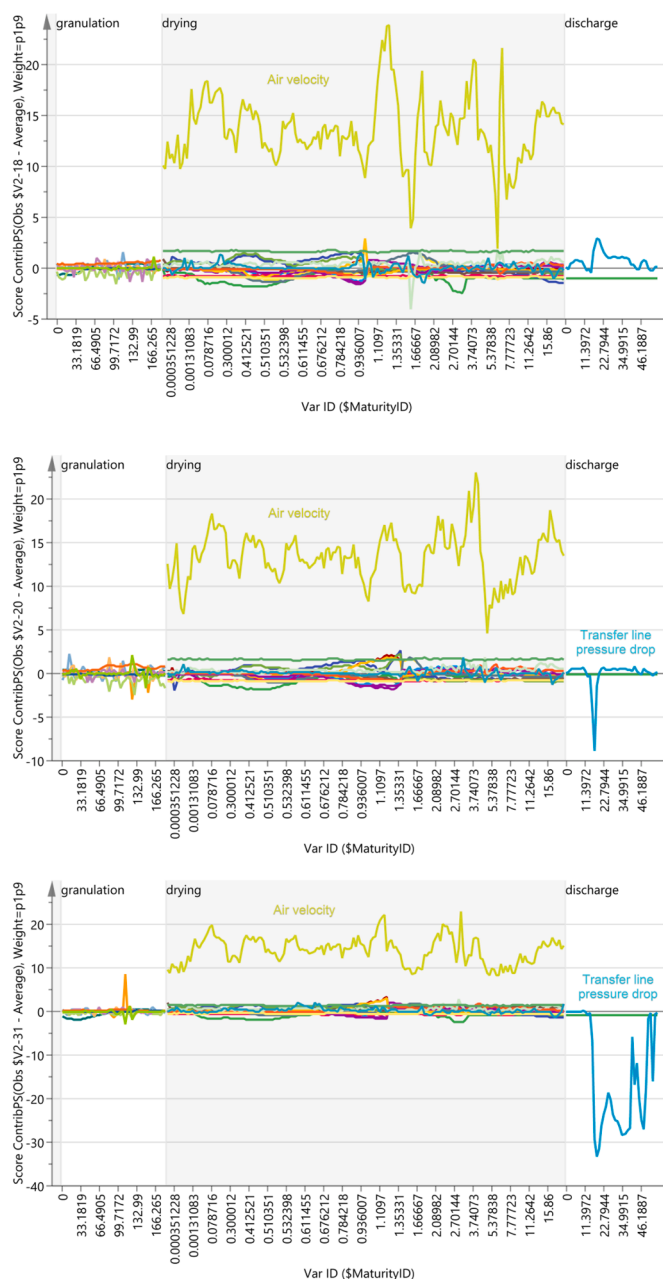


**Fig. 5.** Contribution plot - V2-18 (top), V2-20 (middle) and V2-31 (bottom). The x-axis represents the aligned time series expressed as dryer cell filling time for the granulation, deltaT for the drying phase and discharge time for the discharge phase.

corresponding to the PK of interest. Cell temperatures were therefore renamed as “Temperature cell +0” for the segment where the PK of interest was produced and “Temperature cell +1” to “Temperature cell +5” for the next cells. Finally, the granule discharge is triggered by  $\Delta T$ .  $\Delta T$  is calculated by the equipment only for the next PK to be discharged. In order to obtain the full  $\Delta T$  evolution per PK, this value was recalculated. For each PK the data compiled only consider the phase in which it was in.

For BSP models, the time series data have to be aligned. This alignment aims at allowing the comparison of process trajectories in regard to driving parameters in the process evolution. The granulation step is driven by the dryer cell filling time. The drying step is driven by the  $\Delta T$ . The discharge step is driven by the discharge time. The cell filling time,  $\Delta T$  and discharge time were therefore used for data alignment.

As a result of data pre-processing and filtering, the 3-way process matrix was built. This matrix consisted in J process variables x K time points x N PK. The process matrix was unfolded in such a way that the direction of the J variables was preserved, resulting in a 2-way matrix in which the time and PK dimensions are combined in NxK observations and J variables. A dummy Y vector of length NxK and expressing the local batch time was generated by the software. Three batch evolution models were built: one for the granulation, one for the drying and one for the discharge. Each batch evolution model was developed by regressing local batch time (Y) against the 2-way process matrix (X) via PLS. The variables were scaled to unit variance (UV) and mean-centered prior to modeling. UV-scaling was performed by dividing each value by the standard deviation of that variable and was necessary to normalize for the different numerical ranges of the variables. For mean-centering, the mean of each variable was subtracted from the data of that variable and resulted in a repositioning of the coordinate system, improving the interpretability of the model. The number of PLS components was based on cross-validation as described by Eastment and Krzanowski (1982) but also by assessing the redundancy of information.

After completion of a PK, all data collected for this PK throughout the three phases were used to build a principal component analysis (PCA) model based on the three reference batches. Considering that start-up and shut-down phases may not be at steady state and that the exact number of PK required to reach steady state was unknown, the six first and six last PKs were removed from the reference batches. The PCA model was then built based on 242 PKs from three manufacturing campaigns. Instead of using the original process data from each PK, the scores of the reference batch PLS models were used. The five other manufacturing runs (393 PKs in total) were used to evaluate the model. For this step, all PKs including start-up, shutdown and disturbances were included. The ability of the model to detect start-ups, shutdowns and deviating PKs was assessed using the Hotelling’s  $T^2$  plot, issues reported in the batch records and granules analytical results. The Hotelling’s  $T^2$  plot was selected as this score represents the distance from the model of an observation considering all principal components together. It therefore avoids looking at each principal component individually and is especially relevant for PCA models with many components.

### 3. Results

#### 3.1. Model creation and evaluation

The training set consisted of the process data from the three selected campaigns. Three PLS models were built separately for the granulation, drying and discharge phases. Granulation, drying and discharge data were regressed against the cell filling time,  $\Delta T$  and discharge time respectively. The granulation model resulted in 5 PLS Components (PCs) explaining 78.4% of the dataset variability with no correlation between granulation parameters and filling time ( $R^2Y = 1.0\%$ ). The variability between observations was driven by the feeder parameters (i.e. mass flow in PC1, 2, 4 and 5, screw speed in PC1, 4 and 5), liquid mass flow (PC2 and 4), granulator torque (PC2 and 5), cooling jacket temperature (PC2), barrel temperature (PC3), granulator screw speed (PC4) and wet transfer line flow and pressure drop (PC5). These variations showed no pattern with respect to cell filling time (low  $R^2Y$ ). This result was due to the continuous nature of the granulation step which makes it time independent. The observed variations were due to the oscillations during the process induced by feed-back control loops. The dryer model resulted in 4 PCs explaining 42.3% of the dataset variability. The number of PCs was not further increased as a good correlation between drying parameters and  $\Delta T$  was already achieved with these 4 PCs ( $R^2Y = 87.8\%$ ). The variability between observations was driven by the product temperature in the different cells of the dryer and drying time. The drying process is indeed operating in a discrete flow with a monotonal evolution of product temperature over time. Inlet drying temperature, humidity and air velocity showed limited variation

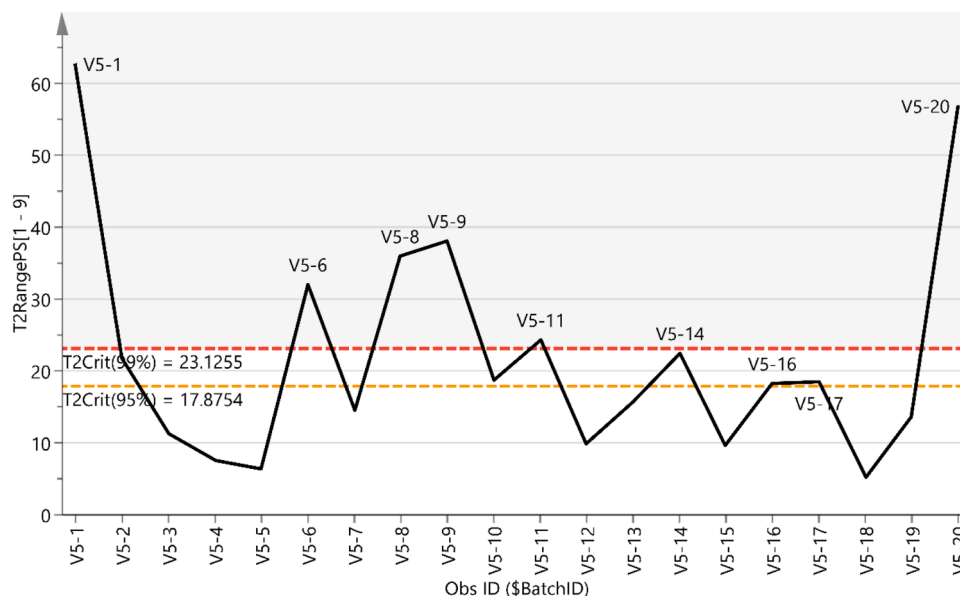


**Fig. 6.** Hotelling's  $T^2$  control charts of test campaign V5. The x-axis represents the sequence of PK per campaign. Deviating PKs are labeled.

between observations as inlet air quality is controlled during the whole process to ensure a constant air quality. The discharge model resulted in 4 PCs explaining 55.0% of the dataset variability with no correlation between discharge parameters and discharge time ( $R^2Y = 13.1\%$ ). The variability between observations was driven by the incoming product drying time (PC1 and 2), discharged dryer cell (PC2 and 4) and pressure drop in the transfer line (PC3). The discharge step, though operating in a discrete flow, does not follow a monotonal evolution over time, making it difficult for PLS to capture its trend as seen with the low  $R^2Y$  value. No variation was observed during the milling step. The milling process was therefore not considered for the rest of the study. These results have already been reported in other studies (Zomer et al., 2018, Silva et al., 2018) and will not be further commented in this article.

The sub-models were then used to build a PCA model allowing to compare PKs. The PCA model was based on the reference batches and consisted of 9 PCs explaining 64.9% of the dataset variability. Five manufacturing runs were tested for fault detection to define the start-up and shut-down phases as well as outlier PKs compared to the reference batches. Hotelling's  $T^2$  values of corresponding PKs were utilized to identify PKs deviating across all PCs (Silva et al., 2017). The Hotelling's  $T^2$  is useful for the identification of strong outliers in the data due to temporary process shifts considering the correlation structure between variables is maintained. The Hotelling's  $T^2$  control chart was created for the test runs.

### 3.2. Verification runs in campaigns without deviations

No issues were reported for campaigns V1, V3 and V4. Campaign V1 was started and immediately stopped by the operator as the pre-blend bin had not been loaded properly. Therefore, the run started at PK2 instead of PK1 and PK1 was not considered. Apart from this minor issue, no deviation was reported in the batch records. The operators reported one pause at PK34. Campaign V3 was paused at PK 46 and restarted. Campaign V4 was paused after PK14 and PK46. Fig. 1 displays the Hotelling's  $T^2$  control charts of test campaigns with start-up, deliberate pause and shut down phases without deviations. The start-up, pauses and shut-down phases were highlighted by the corresponding Hotelling's  $T^2$  control chart and were the only outliers detected by the model. Two PKs were systematically deviating from normal operation during start-up (V1-2 and 3, V3-1 and 2, V4-1 and 2), four during pauses (V1-33 to 36, V3-45 to 48, V4-13 to 15, V4-45 to 48) and one or two

during shut down (V1-101 and 102, V3-90, V4-89 and 90).

The diversion strategy aims at preventing a non-conforming PK to move to the next process step. In the absence of a formal evaluation of the impact of all possible process disturbances on product quality and / or full in-line analysis of product attributes, PKs that are not at steady-state are therefore discarded. As the dryer is composed of six cells operating in parallel, a conservative approach considers that six PKs are needed to achieve steady state. However, discarding six PKs at the beginning and end of each manufacturing campaign can significantly impact the process yield. It is therefore common to only discard the first PK to coat the granulator walls and dryer filters, and to keep the following ones providing that the granule assay is within acceptable ranges. In this case study, the model allowed to identify that the steady state was only achieved for the third PK during start-up and shut down phases. The process dynamics and time to reach steady state indeed depends on process conditions and should be evaluated for each new development.

The contributions plots show the process variables deviating from the calibration set and were therefore used to identify which process parameters deviated during start up and shut down phases. Fig. 2 displays the contributions plot of process parameters deviating from steady state during start-up of test campaigns. During start-up, the feeder starts the screw speed based on feed factor calibration. After 30 s, the control loop adjusts the feeder screws speed (in light blue) based on measured powder feed rate. At the beginning of the campaign, the powder is discharged from the bin and falls of 2 m to the refilling valve of the feeder. The first powder to be fed is therefore denser as it has endured more consolidation leading to the initial feeder screws deviations. The liquid pump then starts (in light purple). The time needed to reach its target value depends on the controller settings and pump settings. In this case, about 70 s were needed for the pump to reach the target liquid feed rate. As the granulator starts empty, the consolidation is low in the barrel leading to a low torque during the two first PKs (in light green). The low torque reflects the limited friction forces inside the granulator barrel (Stauffer et al., 2019). The barrel temperature is then similar to room temperature. The granulator jacket therefore plays the role of a heater rather than of a cooler and the jacket temperature (in orange) is higher than at steady state. At the level of the dryer, only one or two cells are filled during start up. The empty cells temperature (in dark orange, purple, cyan and yellow) are therefore higher than at steady state as no material is present inside them. As these cells are filled, their

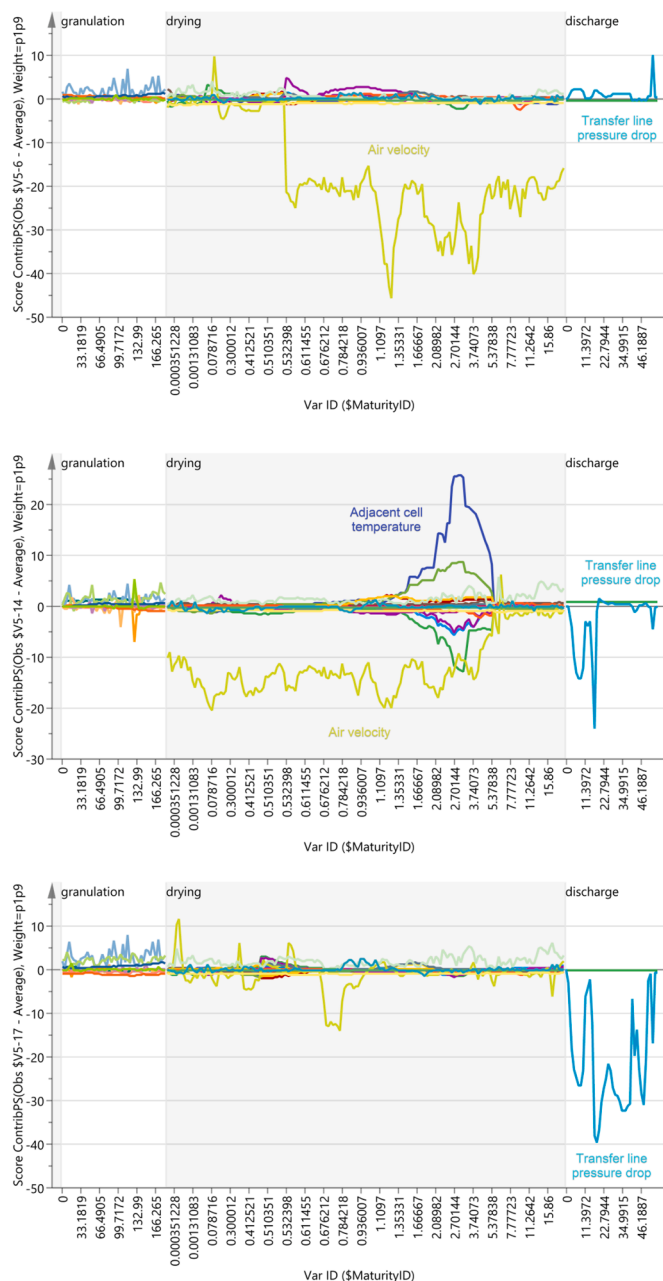


**Fig. 7.** Contribution plot - V5-6 (top), V5-14 (middle) and V5-17 (bottom). The x-axis represents the aligned time series expressed as dryer cell filling time for the granulation,  $\Delta T$  for the drying phase and discharge time for the discharge phase.

temperature slowly goes back to normal operating ranges. As a consequence of partial filling, heat exchange between warm empty cells and filled cold cells allow accelerating the drying of the on-going cells (in green). At the discharge level, the pressure drop within the transfer line (in turquoise) is higher reflecting an easier pneumatic transfer. PK sizes are indeed smaller during start up phases as a portion of the PKs coats the equipment walls and dryer filters and is not discharged.

Fig. 3 displays the contributions plot of process parameters deviating from shut down during test campaigns. During shut down, the refilling of the feeder is stopped to end the manufacturing campaign. The mass in the feeder (in pink) is then lower than at steady state. Due to this lower mass, the feeder controls need to increase feeder screws speed (in light blue) to reach the desired feed rate (Engisch and Muzzio, 2014). At the level of the dryer, the different dryer cells are emptied leading to an

increase of their temperature (in yellow, dark red, gray, dark blue). The drying time of the on-going cell (in green) is accelerated as other cells are emptying. At the discharge level, the pressure drop in the transfer line (in turquoise) is lower compared to steady state reflecting more difficult pneumatic transfer. This might be to the fouling of the filter of the pneumatic transfer line over time.

For these campaigns, the model was able to identify the start-up and shut-down phases on PK level. While it is commonly admitted that the drying process is only formally in steady-state after six cells, it was seen that PK behavior is within normal operating range after the second PK already. The model could therefore be used to rationalize start up and shut down diversion procedure.

### 3.3. Verification runs in campaigns with deviations

Campaign V2 was reported as very challenging by the operators. The drying capacity was reduced due to environmental conditions. In order to achieve sufficiently dried granules, the operators increased the air velocity of  $10 \text{ m}^3/\text{h}$  after PK15. The line was paused at PK25 and restarted at PK26. After restart, turbulent product discharge from the dryer was reported leading to blockage in the pneumatic transfer line at PK31. After this issue, the operators looked closely at the anti-explosion valve of the transfer line and observed a bad positioning of the valve leading to improper discharge. The valve was repositioned at PK32 and the air velocity was reduced to its original value at PK33. No further issue was reported. The corresponding hotelling's  $T^2$  control chart is presented in Fig. 4.

As for Campaigns V1, 4 and 5, start-up and shut down took only two PKs to reach steady state. Apart from these outliers, it was seen that the process deviated from normal operation from PK 15 to PK 32. The contribution plot of each outlier was analysed to identify if the deviation was only due to the change of air velocity by the operator or if other phenomena occurred in parallel to it. From PK15 to 18, the only source of deviation was indeed the inlet air velocity (Fig. 5-top). From PK19 to 21, deviations in the pneumatic transfer line pressure drop were also observed with a maximum deviation observed for PK20 (Fig. 5-middle). The pressure drop strongly decreased for a few seconds at the beginning of product discharge. This deviation was not linked to any alarm and was not noticed by the operators. It was however a herald of the complete blockage observed on PK31 which could have then been prevented by the use of the model. The process was paused between PK25 and 26 resulting in start-up and shut down profiles. Apart from this pause, only the inlet air velocity deviated from normal operation between PK22 and 30. The transfer line blockage observed on PK31 (Fig. 5-bottom) was highlighted by the model with a major decrease of pressure drop compared to normal operation. After repositioning of the valve on PK32 and reduction of the air velocity on PK33, no PK deviated from normal operation until shut down.

Campaign V5 was a shorter technical run performed with an API characterized by a smaller particle size. Multiple issues were reported during this campaign especially a bad fluidization of PK8 and 14 during drying and blockages during pneumatic transfer for PK15 to 17 linked to an obstruction of the transfer line. The corresponding hotelling's  $T^2$  control chart is presented in Fig. 6.

The model identified the start-up (V5-1) and shut down (V5-20) which seemed to be faster for this campaign as only one PK was needed to reach steady state. PK6, 8, 9 and 11 were identified as outliers. PK 14, 16 and 17 were borderline. The model identified outliers that were not reported by the operators (PK6, 9, 11) but could not detect all deviating PK based on observations (PK15 not considered as an outlier and PK14, 16 and 17 as borderline).

The contribution plot of each outlier (based on model and/or on operators' observation) were analysed. A reduction in inlet air flow appeared during PK6 (Fig. 7-top). This air flow deviation was observed in all PKs up to PK14 (Fig. 7-middle) and could explain the fluidization issue reported by the operators. A slight increase in transfer line pressure

drop was also observed just before closing of the transfer line. Considering that most of the PK is discharged within 30 s, this deviation could not be related to product transfer but to the line itself. Drying pattern of adjacent cells deviated from normal operation as exemplified with PK14 (in dark blue in Fig. 7-middle). The deviation in temperature patterns were nonetheless always concomitant with disturbances in air velocity which is impacting not only the fluidization but also the drying kinetics. A decrease in transfer line pressure drop was also observed on PK14 during the opening of the valve and beginning of the discharge (in light blue in Fig. 7-middle). This deviation increased further in the following PKs with a maximum achieved on PK17 (Fig. 7-top). Interestingly, the pneumatic transfer issue appeared when the air velocity deviation stopped, suggesting that both phenomena may be linked. The air velocity in the dryer may indeed impact the discharge rate of the granules via their fluidization regime. After the obstruction identified in the transfer line was found and removed, the last PKs before shutdown showed no deviation from normal operation.

To conclude on these campaigns, the model was able to detect process deviations before issues were noticed by operators. The contribution plots also allowed to understand which process step was deviating and which process parameters were involved, even when these process parameters were not linked to an alarm or when their deviation was below alarm limits.

#### 4. Discussion

Understanding process dynamics is a key aspect for the development of continuous processes. Consigma-25 lines are offering a unique challenge as some unit operations are running in continuous flow (e.g. feeder, granulator) and other unit operations are running in discrete flow (e.g. dryer, discharge, milling). Due to this challenge, previous research on this topic focused either on the continuous flow aspects of the line or only on the discrete unit operations. The quality decision is however taken at PK level for milled granules. The diversion strategy should therefore consider the whole story of an individual PK to ensure only conforming PKs are transferred to the next unit operation.

The methodology described in this paper addresses this gap. The approach allows to trace all process deviations that a PK has encountered within each unit operation. As such, it enables the detection of deviating PKs which can be used for continued process verification, diversion strategy or quality decision.

Current model is however limited to process data. In order to use it for quality decision, the model should be extended with intermediates or final products quality attributes to determine if a deviation is linked to changes in product quality. Raw materials attributes could also be included to relate process deviations to potential change in raw materials. Current model can however be used to select PKs to be analysed to build this knowledge and therefore avoid massive analytical workload to establish process stability. When comparing described methodology to the conservative approach that consists in the systematic sampling of all PKs produced, during campaigns without disturbances (V1, 2 and 3), about 20 PKs would be analysed with this method (outlying PKs and one out of ten conforming PKs) out of the 90–100 PKs produced with the conservative approach. When comparing with a traditional stratified sampling for which the six first PKs, six last PKs and one PK every 10 PK would be analysed, about the same number of analysis would be performed with described methodology, but this methodology ensures to focus the analytical efforts on relevant PKs.

Expanding the current model with intermediate and final product quality attributes would also allow to complement process understanding and to link small and / or short process disturbances with product quality. This is especially meaningful to justify the impact of process excursions that cannot be fully assessed during process development.

Finally, the use this approach for diversion strategy and quality decision would require a full model validation which was not performed in

this study. The combination of current model with on-line analysis and mechanistic models could be beneficial to reach this aim and support quality decision as was reported for MSPC (Dumarey et al., 2019, Domokos et al., 2021). The developed model could then be used as an efficient tool for continued process verification. This is especially valuable as a single model allowed to monitor the different steps of the manufacturing line. The outlier identification could also be used to document the root cause analysis when process deviations are observed.

#### 5. Conclusion

This paper falls in the continuity of previous work performed on the use of multivariate statistical modeling of Consigma 25 manufacturing line. However, while previous studies suggested the possibility to apply batch statistical process monitoring to evaluate individual PKs, they either focused on the full line considering truly continuous variables (e.g. powder feed rate, average product temperature, etc.) or solely on the PK drying trend. In this study, we bridged both approaches to consider the PK as a discrete entity and compare them together. The developed model therefore allowed to identify outlying PKs within a manufacturing campaign. This approach gives new perspectives especially in the context of sampling strategy for development, diversion strategy for non-conforming PKs and continued process verification.

#### CRedit authorship contribution statement

**Fanny Stauffer:** Conceptualization, Methodology, Formal analysis, Investigation, Writing – original draft, Visualization. **Eliot Boulanger:** Formal analysis, Writing – original draft. **Gabrielle Pilcer:** Writing – review & editing.

#### Acknowledgments

The authors would like to thank the manufacturing and analytical teams for their outstanding work during the process development and manufacturing campaigns. A special thanks to Anthony, Fien, Ludivine, Mohammed and Franco from BTO who sweated on the line to master the process.

#### References

- Byrn, S., Futran, M., Thomas, H., Jaycock, E., Maron, N., Meyer, R.F., Myerson, A.S., Thien, M.P., Trout, B.L., 2014. Achieving continuous manufacturing for final dosage formation: challenges and how to meet them. May 20–21. In: 2014 Continuous Symposium, J. Pharm. Sci.. <https://doi.org/10.1002/jps.24247> n/a-n/a.
- De Leersnyder, F., Vanhoorne, V., Bekaert, H., Vercruyse, J., Ghijss, M., Bostijn, N., Verstraeten, M., Cappuyns, P., Van Assche, I., Vander Heyden, Y., Ziemons, E., Remon, J.P., Nopens, I., Vervaet, C., De Beer, T., 2018. Breakage and drying behaviour of granules in a continuous fluid bed dryer: influence of process parameters and wet granule transfer. Eur. J. Pharm. Sci. Off. J. Eur. Fed. Pharm. Sci. 115, 223–232. <https://doi.org/10.1016/j.ejps.2018.01.037>.
- Domokos, A., Pusztai, É., Madarász, L., Nagy, B., Gyürkés, M., Farkas, A., Fülöp, G., Casian, T., Szilágyi, B., Nagy, Z.K., 2021. Combination of PAT and mechanistic modeling tools in a fully continuous powder to granule line: rapid and deep process understanding. Powder Technol. 388, 70–81. <https://doi.org/10.1016/j.powtec.2021.04.059>.
- Dumarey, M., Hermanto, M., Airiau, C., Shapland, P., Robinson, H., Hamilton, P., Berry, M., 2019. Advances in continuous active pharmaceutical ingredient (API) manufacturing: real-time monitoring using multivariate tools. J. Pharm. Innov. 14, 359–372. <https://doi.org/10.1007/s12247-018-9348-7>.
- Eastment, H.T., Krzanowski, W.J., 1982. Cross-validatory choice of the number of components from a principal component analysis. Technometrics 24, 73–77. <https://doi.org/10.2307/1267581>.
- Engisch, W.E., Muzzio, F.J., 2014. Loss-in-weight feeding trials case study: pharmaceutical formulation. J Pharm Innov 10, 56–75. <https://doi.org/10.1007/s12247-014-9206-1>.
- Fonteyne, M., Soares, S., Vercruyse, J., Peeters, E., Burggraef, A., Vervaet, C., Remon, J.P., Sandler, N., De Beer, T., 2012. Prediction of quality attributes of continuously produced granules using complementary pat tools. Eur. J. Pharm. Biopharm. 82, 429–436. <https://doi.org/10.1016/j.ejpb.2012.07.017>.
- Fonteyne, M., Vercruyse, J., Díaz, D.C., Gildemyn, D., Vervaet, C., Remon, J.P., Beer, T. D., 2013. Real-time assessment of critical quality attributes of a continuous

- granulation process. *Pharm. Dev. Technol.* 18, 85–97. <https://doi.org/10.3109/10837450.2011.627869>.
- Food and Drug Administration, 2004. Guidance for Industry PAT — A Framework for Innovative Pharmaceutical Development, Manufacturing, and Quality Assurance. <http://www.fda.gov/downloads/Drugs/Guidances/ucm070305.pdf>.
- Food and Drug Administration, 2019. Guidance For Industry, Quality Considerations For Continuous Manufacturing (draft). Food and Drug Administration.
- International Conference on Harmonisation of Technical Requirements for Registration of Pharmaceuticals for Human Use, 2008. Guidance for Industry Q10, Pharmaceutical Quality System. [http://www.ich.org/fileadmin/Public\\_Web\\_Site/ICH\\_Products/Guidelines/Quality/Q10/Step4/Q10\\_Guideline.pdf](http://www.ich.org/fileadmin/Public_Web_Site/ICH_Products/Guidelines/Quality/Q10/Step4/Q10_Guideline.pdf).
- International Conference on Harmonisation of Technical Requirements for Registration of Pharmaceuticals for Human Use, Requirements for Registration of Pharmaceuticals for Human Use, 2009. Q8(R2): Pharmaceutical Development. <http://www.fda.gov/downloads/Drugs/Guidances/ucm073507.pdf>.
- International Conference on Harmonisation of Technical Requirements for Registration of Pharmaceuticals for Human Use, 2021. Draft ICH guideline Q13 on Continuous Manufacturing of Drug Substances and Drug Products. [https://www.ema.europa.eu/documents/scientific-guideline/draft-ich-guideline-q13-continuous-manufacturing-drug-substances-drug-products-step-2b\\_en.pdf](https://www.ema.europa.eu/documents/scientific-guideline/draft-ich-guideline-q13-continuous-manufacturing-drug-substances-drug-products-step-2b_en.pdf).
- Lee, S.L., O'Connor, T.F., Yang, X., Cruz, C.N., Chatterjee, S., Madurawe, R.D., Moore, C. M.V., Yu, L.X., Woodcock, J., 2015. Modernizing pharmaceutical manufacturing: from batch to continuous production. *J. Pharm. Innov.* 10, 191–199. <https://doi.org/10.1007/s12247-015-9215-8>.
- Plumb, K., 2005. Continuous processing in the pharmaceutical industry: changing the mind set. *Chem. Eng. Res. Des.* 83, 730–738. <https://doi.org/10.1205/cherd.04359>.
- Roggo, Y., Pauli, V., Jelsch, M., Pellegatti, L., Elbaz, F., Ensslin, S., Kleinebudde, P., Krumme, M., 2020. Continuous manufacturing process monitoring of pharmaceutical solid dosage form: a case study. *J. Pharm. Biomed. Anal.* 179, 112971 <https://doi.org/10.1016/j.jpba.2019.112971>.
- Silva, A.F., Sarraguça, M.C., Fonteyne, M., Vercruyse, J., De Leersnyder, F., Vanhoorne, V., Bostijn, N., Verstraeten, M., Vervaet, C., Remon, J.P., De Beer, T., Lopes, J.A., 2017. Multivariate statistical process control of a continuous pharmaceutical twin-screw granulation and fluid bed drying process. *Int. J. Pharm.* 528, 242–252. <https://doi.org/10.1016/j.ijpharm.2017.05.075>.
- Silva, A.F., Vercruyse, J., Vervaet, C., Remon, J.P., Lopes, J.A., De Beer, T., Sarraguça, M.C., 2018. Process monitoring and evaluation of a continuous pharmaceutical twin-screw granulation and drying process using multivariate data analysis. *Eur. J. Pharm. Biopharm.* 128, 36–47. <https://doi.org/10.1016/j.ejpb.2018.04.011>.
- Stauffer, F., Ryckaert, A., Van Hauwermeiren, D., Funke, A., Djuric, D., Nopens, I., De Beer, T., 2019b. Heat transfer evaluation during twin-screw wet granulation in view of detailed process understanding. *AAPS PharmSciTech* 20, 291. <https://doi.org/10.1208/s12249-019-1483-z>.
- Stauffer, F., Vanhoorne, V., Pilcer, G., Chavez, P.-F., Vervaet, C., De Beer, T., 2019a. Managing API raw material variability in a continuous manufacturing line – Prediction of process robustness. *Int. J. Pharm.* 569, 118525 <https://doi.org/10.1016/j.ijpharm.2019.118525>.
- Vanhoorne, V., Vervaet, C., 2020. Recent progress in continuous manufacturing of oral solid dosage forms. *Int. J. Pharm.* 579, 119194 <https://doi.org/10.1016/j.ijpharm.2020.119194>.
- Vercruyse, J., Córdoba Díaz, D., Peeters, E., Fonteyne, M., Delaet, U., Van Assche, I., De Beer, T., Remon, J.P., Vervaet, C., 2012. Continuous twin screw granulation: influence of process variables on granule and tablet quality. *Eur. J. Pharm. Biopharm.* 82, 205–211. <https://doi.org/10.1016/j.ejpb.2012.05.010>.
- Vercruyse, J., Delaet, U., Van Assche, I., Cappuyns, P., Arata, F., Caporicci, G., De Beer, T., Remon, J.P., Vervaet, C., 2013. Stability and repeatability of a continuous twin screw granulation and drying system. *Eur. J. Pharm. Biopharm.* 85, 1031–1038. <https://doi.org/10.1016/j.ejpb.2013.05.002>.
- Vervaet, C., Vercruyse, J., Remon, J.P., Beer, T.D., 2013. Continuous processing of pharmaceuticals. *Encycl. Pharm. Sci. Technol.* Fourth Ed. Taylor & Francis, pp. 644–655. <http://www.tandfonline.com/doi/abs/10.1081/E-EPT4-120050224> (accessed February 16, 2015).
- Zomer, S., Zhang, J., Talwar, S., Chatteraj, S., Hewitt, C., 2018. Multivariate monitoring for the industrialisation of a continuous wet granulation tableting process. *Int. J. Pharm.* 547, 506–519. <https://doi.org/10.1016/j.ijpharm.2018.06.034>.